ENGINEER - Vol. LVIII, No. 01, pp. [97-107], 2025
© The Institution of Engineers, Sri Lanka
DOI: https://doi.org/10.4038/engineer.v58i1.7681

Probabilistic Liquefaction Potential Approach for Colombo Port City

I.A.C.C. Ilangakoon and A.M.R.G. Athapaththu

Abstract: The Colombo Port City, Sri Lanka's major coastal project, has been constructed by transforming 269 hectares of sea into a vibrant residential, retail, and business land area using 65 million cubic meters of dredged sand. Coastal areas undergoing land reclamation often face challenges related to liquefaction, primarily induced by natural seismic events. Recent studies underscore the importance of considering seismic events during the design phase of construction projects in Sri Lanka. This paper describes a study that performed probabilistic liquefaction hazard analyses using a well-established method. To investigate surface damage potential, the Liquefaction Potential Index method was employed. Detailed analysis of the results was used to develop maps illustrating liquefaction behaviour with depth, providing a comprehensive assessment of the potential for ground liquefaction. The comparison of the two methods indicates that, out of the four earthquake combinations considered, two scenarios are particularly critical. Additionally, certain land plots have been identified as more vulnerable to liquefaction.

Keywords: Colombo Port City, Land reclamation, Liquefaction, Probabilistic, Liquefaction Potential Index

1. Introduction

Liquefaction refers to a process in which saturated, cohesion-less soils, particularly sand, lose their strength and stiffness due to applied stresses, such as earthquakes, resulting in significant deformation or flow. The term originated from Hazen (1918), who used it to describe the failure of a hydraulic fill dam. Later, researchers like Casagrande (1979) and Seed (1979) expanded its definition, describing liquefaction as a condition where loose, saturated sands lose strength due to high pore-water pressures, which reduce effective confining pressure.

Interest in liquefaction grew after the June 16, 1964, Niigata earthquake in Japan, as it caused significant structural damage and highlighted the phenomenon's potential impact (Seed & Idriss, 1967). Before this event, liquefaction was poorly understood. Following the earthquake, Terzaghi and Peck (1967) introduced the term “spontaneous liquefaction” to describe the sudden loss of strength in very loose, saturated sands due to disturbances.

Robertson and Wride (1998) further elaborated on the theory, explaining that during seismic events, saturated soils can generate high pore water pressures, reducing effective stress to near zero. If cyclic loading, such as from an earthquake, continues, the soil undergoes increased deformation. Two types of soil liquefaction were identified: flow liquefaction, triggered by static or dynamic loads disrupting soil equilibrium, and cyclic softening liquefaction, caused by cyclic loading, which is the more common form, affecting both flat and inclined grounds.

Multiple methodologies exist for assessing liquefaction potential, including probability of liquefaction (probabilistic approach), Factor of Safety (FOS), Liquefaction Potential Index (LPI), and liquefaction-induced settlement. This paper describes a study evaluating the liquefaction potential of the Colombo Port City premises using the probabilistic approach.

In the liquefaction potential evaluation, probabilistic and LPI methods incorporate the FOS values that are calculated against liquefaction failure.

Eng. I.A.C.C. Ilangakoon, AMIE(SL), B.Sc. Eng.(SLIIT), MScEng (Peradeniya), Senior Civil Engineer, Civil & Structural Engineering Consultants (Pvt) Limited, Sri Lanka
Email:Charith.ilangakoon@gmail.com
ORCID ID: https://orcid.org/0009-0008-4264-4775
Eng. (Dr.) A.M.R.G. Athapaththu, AMIE(SL), B.Sc.Eng. (Peradeniya), MPhil (Peradeniya), DEng (Hiroshima)
Senior Lecturer, Department of Civil Engineering, University of Peradeniya, Peradeniya
Email:Rasika@eng.pdn.ac.lk
ORCID ID: https://orcid.org/0000-0001-9342-2189

Probabilistic approach is widely utilized globally due to its effectiveness in illustrating outcomes (Juang & Jiang, 2000). To determine the FOS, scientists worldwide have devised several methodologies, among which empirical correlations and the 'Simplified Procedure,' introduced by Seed and Idriss (1971), are commonly employed. This study adopts the simplified procedure developed by Seed and Idriss, deemed the most convenient method. Seed and Idriss described a soil column as a rigid body affected by seismic forces at its base, causing shear waves to move toward the ground surface. The resulting shear stress in the soil was calculated using empirical formulas.

However, the simplified procedure is not without its limitations. The probabilistic approach, which is based on the simplified method, while broadly applicable, may sometimes overlook factors such as the fabric of the soil structure. Cone Penetration Test (CPT) and Standard Penetration Test (SPT) values, which are used in the simplified method, primarily represent soil density. Liquefaction potential depends not only on density but also on the fabric of the soil structures. Consequently, these methodologies might not always provide completely accurate results in all scenarios.

The study analyses geotechnical investigation data from CPTs using a CPT-based simplified liquefaction assessment method for free-field level ground conditions. It aims to determine the liquefaction potential of the Colombo Port City by evaluating the probability of liquefaction and the Liquefaction Potential Index (LPI). The analysis considers four different earthquake combinations, accounting for the seismicity around the island.

Results are presented as probability of liquefaction contours at various depths beneath the ground surface, along with spatial distribution contours outlining the LPI.

2. Liquefaction Process and Structural Vulnerabilities in Colombo Port City

The primary cause of liquefaction is typically natural seismic events, although rare manmade incidents can also trigger sudden liquefaction. Liquefaction can be defined as the process where rapid loading on saturated soil layers during earthquakes causes a significant increase in pore-water pressure, which leads to a reduction in effective stress. When the effective stress approaches near zero, the soil transitions from a solid state to a liquid state. This transformation results in the collapse of loosely packed particles and insufficient time for excess pore-water pressure to dissipate, causing a substantial decrease in soil strength, stiffness, and volume. Hazen (1918) provides a clear explanation of the process of soil liquefaction for better understanding.

Liquefaction events can cause various ground failures, including sand boiling, flow failure, lateral spreading, vertical settlement, and loss of bearing strength. Flow failure, characterized by rapid soil displacement, is the most recognized form of ground collapse induced by liquefaction (Ishihara, 1993). Lateral spread failure involves the lateral displacement of liquefied soil due to seismic forces. In flat areas or gentle slopes, liquefaction at greater depths can lead to the decoupling of soil layers, causing ground oscillations. Liquefied ground is vulnerable to lateral spread failure on slopes steeper than 3 degrees (Youd & Perkins, 1978). Sand boiling occurs at liquefied sand surfaces, especially when surrounded by hardened ground with weak spots. Soil liquefaction primarily impacts structures on saturated sandy soils or piles, causing differential settlement and potential damage to buried utilities.

Historically, major liquefaction incidents such as the 1964 Niigata earthquake in Japan (Seed & Idriss, 1967), the 2011 Great East Japan Earthquake (Yasuda et al., 2012), the 2010-2011 earthquakes in Christchurch, New Zealand (Cubrinovski et al., 2010), the 1989 Loma Prieta earthquake in San Francisco (Kayen et al., 1992), and the 1999 Chi-Chi earthquake in Taiwan (Juang et al., 2002) have resulted in severe consequences. These consequences include settlement failures, bearing failures, tilting failures, and lateral movements, primarily affecting reclaimed land.

Various effects are foreseeable during earthquake-induced soil liquefaction events in Colombo Port City, particularly for low-rise structures like highway structures, swimming pools, playgrounds, and buildings with shallow foundations. Highway structures may experience sudden support loss, while irregular ground settlement can damage underground utilities such as water, sewer, and gas pipelines, and allow water infiltration into buildings, potentially causing structural damage.

3. Evaluation of Factor of Safety

Soil liquefaction predominantly hinges on earthquake magnitude, ground motion intensity and duration, ground acceleration, soil density, effective confining pressure, soil layer thickness, fines content, groundwater table position, and reduction of effective stress (Youd & Perkins, 1978). These parameters can be simplified into two factors: the intensity of seismic loading (Cyclic Stress Ratio, CSR) and the characterization of liquefaction resistance (Cyclic Resistance Ratio, CRR) of the soil. By comparing CSR and CRR, it is possible to assess the likelihood of liquefaction occurrence at any particular depth at a site.

3.1. Cyclic Stress Ratio (CSR)

Peak Ground Acceleration (PGA), which depends on site-specific ground motion, can be utilized to calculate CSR. The equation for CSR induced by earthquake ground motions, formulated by Seed and Idriss (1971), is presented in Equation No. 1.

$$CSR = 0.65\left(\frac{\sigma_v}{\sigma'_v}\right)\left(\frac{a_{max}}{g}\right)r_d \qquad \ldots(1)$$

where,

σ_v = Total stress at the depth Z
σ'_v = Effective stress at the depth Z
g = Acceleration of gravity
a_{max} = Peak ground acceleration
r_d = Shear stress reduction factor for depth Z given by,

$$r_d = \begin{cases} 1.0 - 0.00765z, & z \leq 9.15m \\ 1.174 - 0.0267z, & 9.15 < z \leq 23m \end{cases} \qquad \ldots(2)$$

In actual situations, the soil behaves more like a flexible body rather than a rigid one. Equation No. 1 adjusts the rigid body shear stress by a Stress Reduction factor (r_d) (Equation No. 2), as proposed by Seed and Idriss (1971), to account for this flexibility and obtain the deformable body shear stress with depth. A factor of 0.65 is applied to reduce the maximum shear stress, ensuring reasonable accuracy in the calculation procedure. Originally, this simplified equation was developed for earthquakes of magnitude 7.5. To adapt it to different magnitudes, a variable known as the "Magnitude Scaling Factor" (MSF) must be considered. The MSF values suggested by Seed and Idriss (1982) were used for the calculations in this study, as outlined in Equation No. 3.

$$MSF = \left(\frac{Mw}{7.5}\right)^n \; ; n = -2.56 \qquad \ldots(3)$$

where,

MSF = Magnitude Scaling Factor
Mw = Magnitude of the Earthquake
n = Constant

The final version of CSR used in this study was computed as depicted in Equation No. 4, after considering all relevant factors.

$$CSR = 0.65\left(\frac{\sigma_v}{\sigma'_v}\right)\left(\frac{a_{max}}{g}\right)\frac{r_d}{MSF} \qquad \ldots(4)$$

3.2. Cyclic Resistance Ratio (CRR)

CPT is widely used in assessing the liquefaction potential of sandy soils. It offers a detailed soil profile, which helps in evaluating liquefaction resistance. After the introduction of simplified liquefaction analysis, various CPT-based methods have emerged. Among them, the Robertson method developed by Robertson and Wride (1998), has gained global recognition for its reliability and widespread application.

Robertson and Wride (1998) devised an approach that addresses the limitations of other techniques. Key factors in the Robertson method include the soil behaviour type index (Ic), Equivalent Clean Sand Normalized CPT Penetration Resistance (Qc1N,cs), correction factor for the grain characteristics of the soil (Kc), Normalized CPT Penetration Resistance (Q), Normalized Friction Ratio (Fs), and the CRR profile for an earthquake of magnitude (M) equal to 7.5, referred to as $CRR_{7.5}$.

The reclaimed sand used in the Colombo Port City was identified as not clean, and the necessary corrections to Qc1N,cs were applied in accordance with Robertson and Wride's (1998) method prior to calculating the CRR. Robertson and Wride (1998) suggested a flow chart approach for calculating the CRR of sandy soils using the CPT-based method. The flow chart employed in this study for the calculation is described in detail by Robertson and Wride (1998).

3.3. Factor of Safety

The Factor of Safety (FOS) against soil liquefaction can be estimated once the values of CSR and CRR have been obtained for a soil layer at a specific depth. Equation No. 5 represents the formula for calculating the FOS against liquefaction. The evaluation of liquefaction based on the factor of safety method is illustrated in detail, along with a sample calculation, by Ilangakoon and Athapaththu (2023).

$$\mathrm{FOS} = \frac{\mathrm{CRR}}{\mathrm{CSR}} \qquad \ldots(5)$$

4. Probabilistic Liquefaction Assessment Approach

A significant limitation of the simplified procedure is that, it only yields the FOS as an outcome. While conventional thinking suggests that liquefaction occurs when FOS is less than 1 and does not occur when FOS is greater than 1, there are instances where liquefaction still happens even with FOS greater than 1 (Seed et al., 1985 & Liao et al., 1988). Therefore, researchers have aimed to examine the caution of proposed CRR models. Juang and Jiang (2000) developed a mapping function, depicted in Equation No. 6, to evaluate the importance of the estimated FOS values in terms of the likelihood of liquefaction occurring, following the research by Chen and Juang (2000). This mapping function converts the FOS values into a percentage probability of liquefaction, offering a more nuanced understanding of liquefaction risk. A and B in the equations are referred to as Mapping Functions, and the respective values for the selected method are shown in Table 1.

$$\mathrm{P_L} = \frac{1}{1 + \left(\frac{\mathrm{F_s}}{A}\right)^{B}} \% \qquad \ldots(6)$$

where,

A & B = Mapping Functions
F_s = Factor of Safety
P_L = Probability of Liquefaction

Table 1 - Mapping Function Values for Selected Method (Juang & Jiang, 2000)

Method	A	B
Robertson Method	1.00	3.3

Instead of being bound to a numerical design approach, this method can serve as a foundation for a risk-based design strategy to mitigate liquefaction potential (Chen & Juang, 2000). In engineering practice, soil failure is often defined as occurring when there is a liquefaction probability exceeding 50% (Juang et al., 2002). In this paper, for easier interpretation of the results, these values have been converted to percentages. This conversion allows for a more intuitive understanding of the data.

5. Liquefaction Potential Index

The Liquefaction Potential Index (LPI) measures the severity of liquefaction and predicts surface manifestations, damage, or the likelihood of failure in liquefaction-prone areas. The LPI method is primarily used in areas with a high risk of liquefaction to assess liquefaction potential (Fukutake & Yamamoto, 1996). However, this approach only provides a simplified visualization of a site's potential for liquefaction.

Iwasaki et al. (1978) introduced LPI as a means to quantify the likelihood of liquefaction. The methodology proposed by Iwasaki et al. (1978) involves an indicator that correlates with the thickness and FOS against liquefaction for each soil layer, obtainable through conventional methods. Soil layers with an FOS greater than 1.2 are categorized as non-liquefied, those with FOS between 1.0 and 1.2 are classified as marginally liquefiable, and those with a FOS below 1.0 are considered liquefiable.

A weighting formula assigns higher values to layers closer to the ground surface, linearly decreasing in value down to a depth of 20 meters (Iwasaki et al., 1982). However, reliance solely on FOS obtained through standard techniques is inadequate for assessing liquefaction potential due to uncertainties related to geological and seismological conditions, fines content, and in-situ testing (such as SPT, CPT, and Shear Wave Velocity (Vs)). Seed and Idriss (1982) consider FOS values between 1.25 and 1.5 acceptable for non-liquefied soils. In response, Sonmez (2003) adjusted the Iwasaki et al. (1978) method, assuming a FOS of 1.2 for the lowest value of the liquefaction potential category, aligning with the acceptable values for non-liquefied soil suggested by Seed and Idriss (1982). Sonmez (2003) modified the original equations proposed by Iwasaki et al. (1978) for the Liquefaction Potential Index, resulting in Equation Nos. 7 to 13.

$$LPI = \int_0^{20} F(z)W(z)\,dz \qquad \ldots(7)$$

$$LPI = \int_0^{20} F(z)(10 - 0.5z)\,dz \qquad \ldots(8)$$

$$F(z) = 0 \quad for\ FOS \geq 1.2 \qquad \ldots(9)$$

$$F(z) = 2\,(10^6)\,(e^{-18.427*FOS}) \quad for\ 1.2 > FOS > 0.95 \qquad \ldots(10)$$

$$F(z) = 1 - FOS \quad for \quad FOS < 0.95 \qquad \ldots(11)$$

$$W(z) = 0 \quad for\ Z > 20\,m \qquad \ldots(12)$$

$$W(z) = 10 - 0.5z \quad for\ Z \leq 20\,m \qquad \ldots(13)$$

where,
F = Safety factor of each layer
W = Depth weighting factor of each layer
Z = Thickness of each layer

Additionally, the liquefaction potential categories defined by Iwasaki et al. (1978) were reorganized to address identified limitations and constraints, as shown in Table 2. The extremely low category was eliminated, and the non-liquid and neutral categories were introduced. The lower category of the original classification model was subdivided into moderate and low subcategories. The boundaries of LPI values for the categories were adjusted accordingly, while the high and very high boundary LPI values remained unchanged.

Table 2 - Categorization of Severity of Liquefaction Damage (Iwasaki et al., 1978)

Liquefaction Potential Index	Severity of Liquefaction
0	Very Low
0<LPI ≤5	Low
5<LPI ≤15	High
15≥ LPI	Very High

The modified LPI evaluation approach was utilized in this research to calculate the liquefaction potential index.

6. Selection of Input Ground Motions

The seismic scenario surrounding Sri Lanka, as utilized in Ilangakoon and Athapaththu (2023), was selected for the present analyses, with a focus on earthquakes originating in the sea and considering the impact of earthquake magnitude and distance. The selected seismic scenarios, based on previous studies, include a controlling and critical earthquake with a magnitude of 6.9, a 475-year return period, and an epicentral distance of 90 km, situated along the failed Mannar rift zone and Comorin ridge (Seneviratne et al., 2020). A second earthquake scenario with a magnitude of 7.5 was chosen to examine the impacts of a larger-magnitude earthquake at the same epicentral distance (Seneviratne, 2016). The same combination used in the study by Kumarasiri and Abayakoon (2008) was chosen as the third design earthquake combination, involving a magnitude 6.0 earthquake with an acceleration of 0.2. The fourth earthquake combination, a magnitude 6.9 earthquake with an acceleration of 0.2, was chosen for its highest values considering the past literature (Kumarasiri & Abayakoon, 2008). Earthquakes with magnitudes lower than the critical earthquake but generated at closer distances (M = 6.0 earthquake with an epicentral distance of 15 km) were excluded from this study, as they showed minimal liquefaction effects on the Colombo Port City in Ilangakoon and Athapaththu (2023). These combinations, included in Table 3, summarize the seismic scenarios anticipated within the island used for this study.

Table 3 - Seismic Combinations for the Study

Combination	Magnitude	PGA Value
1	6.9	0.1
2	7.5	0.1
3	6.0	0.2
4	6.9	0.2

7. Study Area Considered in the Research

This project is located in a coastal area where the dredged sand fill layer exceeds 13 meters in thickness. The Colombo Port City is partitioned into two construction phases: Phase 1, designated for high-rise structures, and Phase 2, intended for mid-rise residential buildings and open spaces. Preceding construction, Phase 1 and a portion of Phase 2 underwent enhancement using vibro-flotation and dynamic compaction methods. These phases are subdivided into 14 land plots. The majority of CPT boreholes are concentrated in areas designated for roadways and high-rise buildings.

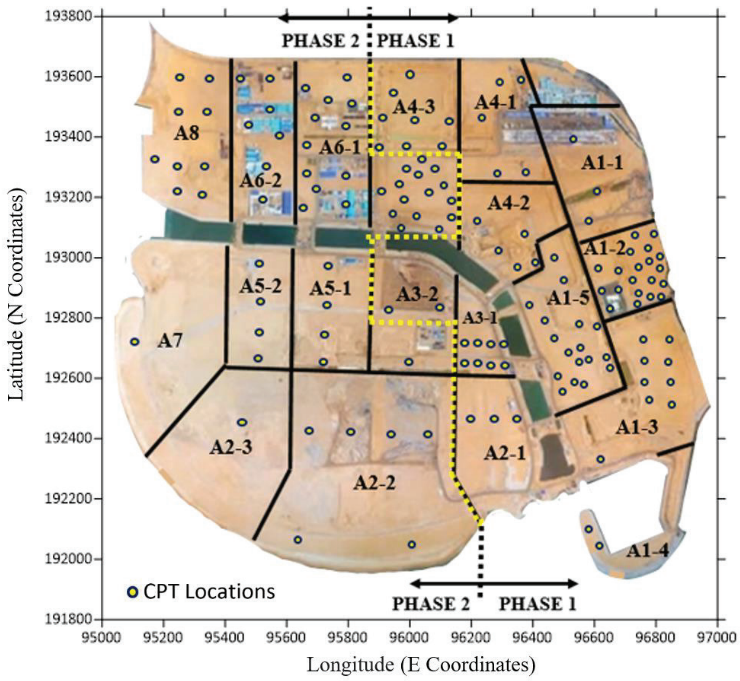

Figure 1 - Aerial View of Colombo Port City Showing Reclamation Land Plots, Main Construction Phases, and Locations of the 142 CPTs Selected

Analysis of CPT borehole records from 142 representative locations across the city was conducted to assess liquefaction potential, spanning depths of 8m to 23m. An aerial view of Colombo Port City, displaying CPT locations and construction phases, is presented in Figure 1.

8. Engineering Implications

This study employs a CPT-based simplified method to assess the liquefaction probability for the worst-case seismic scenarios in the high-priority area of Colombo Port City. Contour maps depicting liquefaction probability values at depths of 6 m, 12 m, and 17 m were developed to identify liquefaction-susceptible zones, with nearly all locations exhibiting a notable increase in probability values with increasing depth. Figures 2, 3, 4, and 5 illustrate the contour maps for the CPT-based probabilistic liquefaction analysis assessment carried out at different depth profiles for earthquake combinations 1, 2, 3, and 4, respectively.

To develop the liquefaction probability contours, calculations and analyses were performed for each level at all CPT locations.

Three specific depths were selected to elaborate on the results: 6 m, 12 m, and 17 m. These depths were chosen to provide a detailed representation of liquefaction potential at varying subsurface levels.

The contours were generated using "SURFER - Golden Software," a specialized tool for geospatial data visualization. However, due to the limitations of the software, it was not possible to restrict the contour lines exclusively to the land area of the Port City map. Consequently, the contours extended into the adjacent sea area during the visualization process.

It is important to note that CPTs were conducted only in the reclaimed land areas and none in the sea areas. As a result, the liquefaction probabilities displayed in the sea area are not based on actual data and should not be considered accurate or valid. This extension into the sea area is purely illustrative and should not be interpreted as an analysis of seabed conditions.

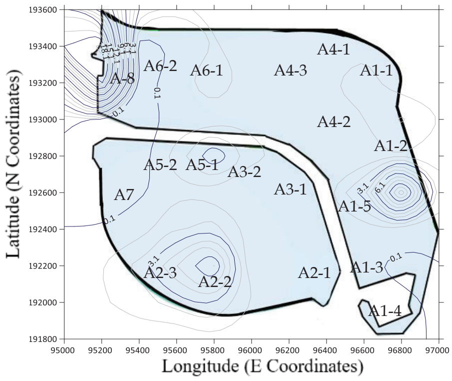

(a)

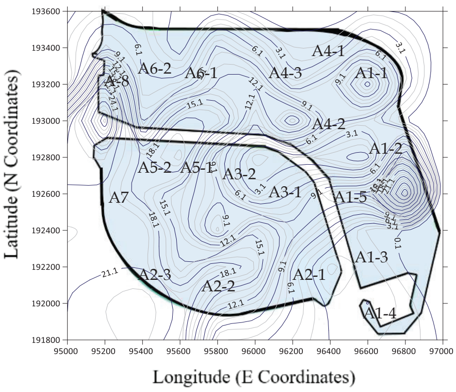

(b)

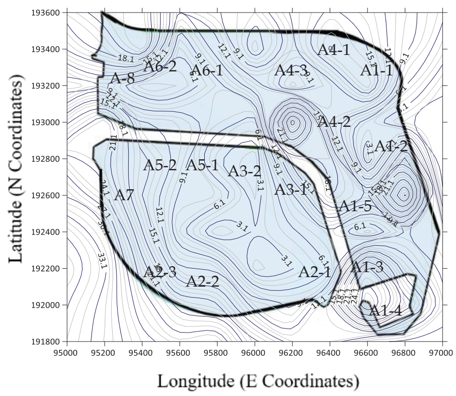

(c)

Figure 2 - Contours of Probability of Liquefaction for Combination 1, (a) at a Depth of 6 m; (b) at a depth of 12 m; (c) at a depth of 17 m.

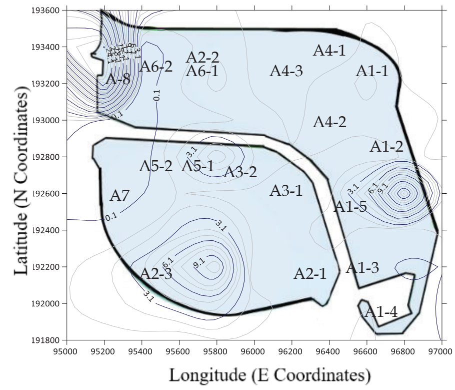

(a)

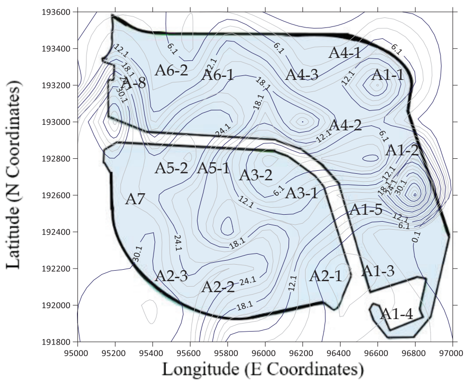

(b)

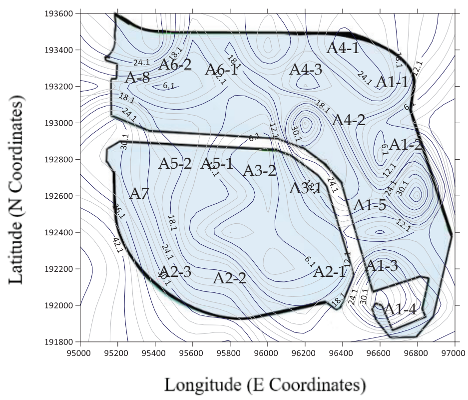

(c)

Figure 3: Contours of Probability of Liquefaction for Combination 2, (a) at a Depth of 6 m; (b) at a Depth of 12 m; (c) at a Depth of 17 m.

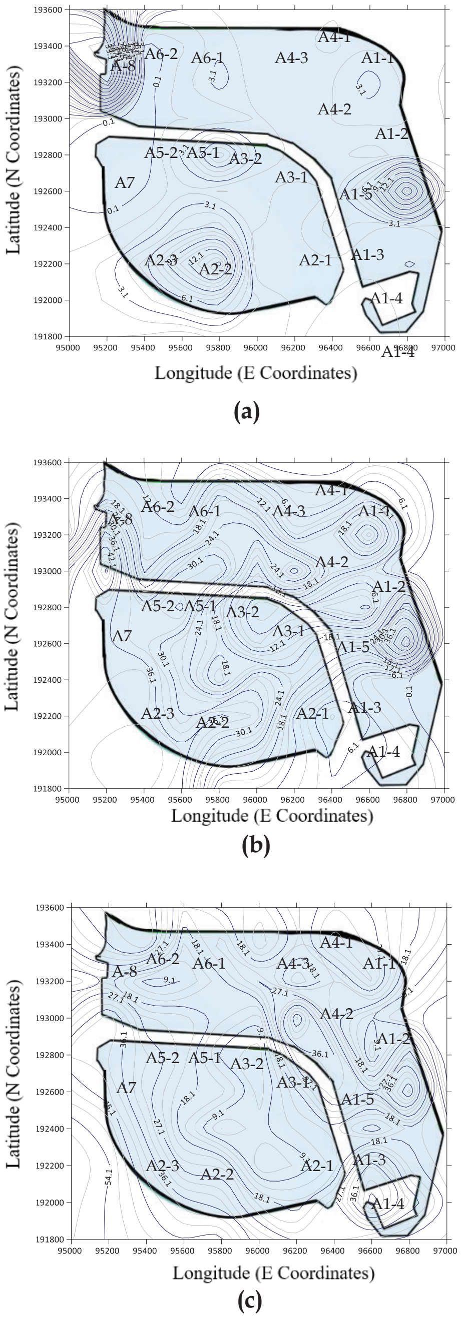

Figure 4 - Contours of probability of liquefaction for combination 3, (a) at a depth of 6 m; (b) at a depth of 12 m; (c) at a depth of 17 m.

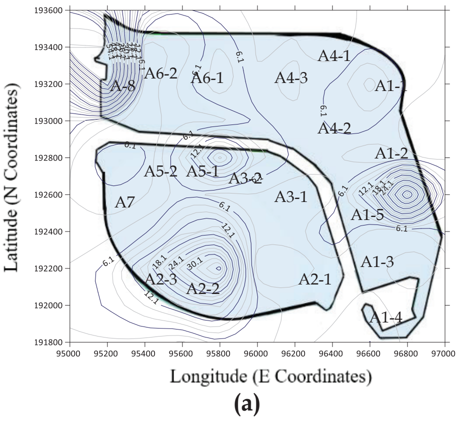

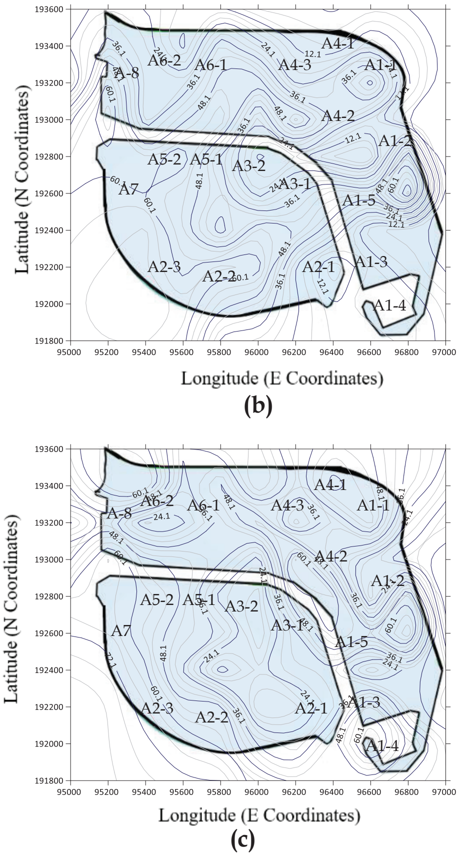

Figure 5 - Contours of probability of liquefaction for combination 4, (a) at a depth of 6 m; (b) at a depth of 12 m; (c) at a depth of 17 m.

These contour maps depict the geographic variation in liquefaction effects and potential surface manifestations. They emphasize the susceptibility of Colombo Port City to liquefaction, especially in areas where the probability exceeds 50%. Land plots A8, A6-2, A6-1, A5-2, A3-2, A4-3 and A5-1 are identified as highly vulnerable to severe liquefaction in earthquake scenarios 2, 3, and 4. The study concludes that certain land plots in Phase 02 of Colombo Port City are at high risk of soil liquefaction, particularly when earthquake magnitude exceeds 6.0 and acceleration values exceed 0.2g. Conversely, liquefaction in Phase 01 is deemed extremely unlikely.

For all four earthquake scenarios, the Probability of Liquefaction values at a depth of 6 m are notably lower compared to those at 12 m and 17 m depths. This difference is likely attributed to the effectiveness of ground improvement measures, which primarily extend to shallow depths. The Probability of Liquefaction values at a depth of 17 m are similar to those at 12 m, though some locations show slightly higher values at 17 m.

Furthermore, Figure 6 illustrates the developed contour maps for the LPI analysis, indicating that Phase 2 of the Colombo Port City development project may contain some weak strata. The LPI analysis helps to identify specific land plots with a high potential for liquefaction, including plots A8, A6-2, A6-1, A5-2, and A5-1.

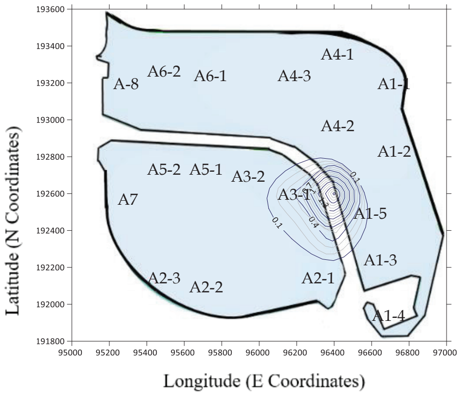

(a)

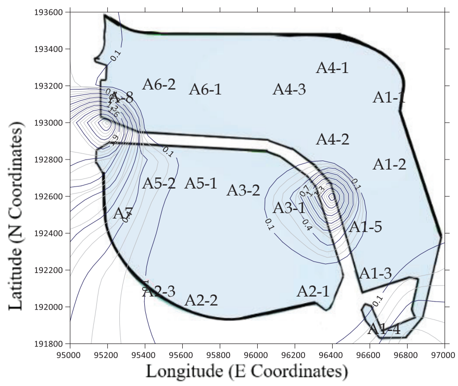

(b)

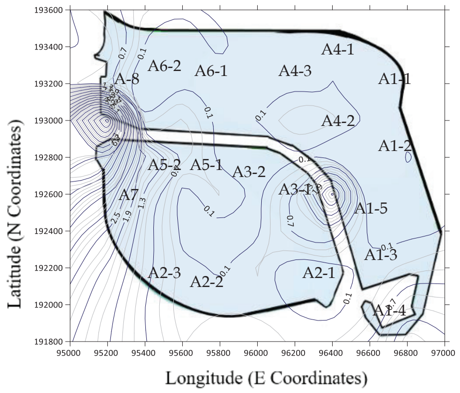

(c)

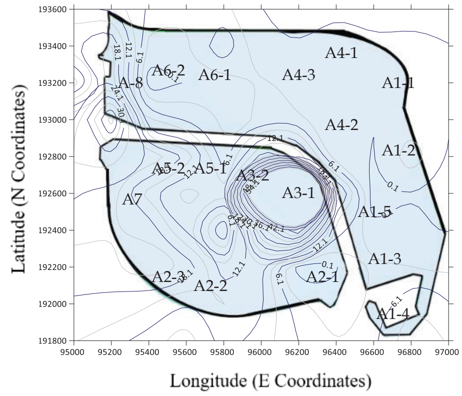

(d)

Figure 6 - Contours of liquefaction potential index (LPI) values, (a) For combination 01; (b) For combination 02; (c) For combination 03; (d) For combination 04.

9. Conclusions

In the present study, liquefaction triggering analysis was conducted through the probability of liquefaction and Liquefaction Potential Index (LPI) using CPT-based simplified methods for free-field level ground conditions.

These contour maps will aid designers, engineers, and planners in assessing the vulnerability of the area to liquefaction. They can be effectively utilized for future seismic safety plans and seismic hazard mitigation programs. Additionally, these maps can serve as valuable resources for future studies on liquefaction within the country.

It was observed that critical layers in some CPT locations have a high likelihood of triggering liquefaction, with probability values exceeding 50%. The same land plots were identified as liquefaction-prone through LPI analysis. The earthquake scenarios with Mw = 6.9, PGA = 0.2 and Mw = 6.0, PGA = 0.2 were found to be the most critical in terms of LPI and liquefaction triggering locations among the four anticipated seismic combinations. As previously mentioned, all three approaches exhibit the same pattern of Probability of Liquefaction fluctuation with depth. Sites with a Probability of Liquefaction greater than 50% are particularly susceptible. For earthquake combinations 4 and 5, some city land plots—specifically A8, A6-2, A6-1, A5-2, and A5-1—are highly vulnerable to severe liquefaction and should be considered when designing construction to mitigate the risk of liquefaction. These results could be taken into consideration by city planners if the structures built on these areas are built on shallow foundations, or if they include highway structures, water-retaining structures, or critical utility supply lines, especially given the long lifespan of these structures. Therefore, these earthquake combinations are suitable for future assessments and design work for the Port City of Colombo or other reclamation projects in and around Colombo.

Based on the research findings, several recommendations can be made. While the number of boreholes considered is sufficient to identify liquefaction-prone zones, incorporating new data would allow for more accurate zone demarcation. It is recommended to establish connections with international seismic monitoring stations to obtain better understanding and updates on earthquakes in the region, as records of earth tremors and seismic information are not readily available in Sri Lanka. Lastly, conducting a computer simulation of liquefaction triggering within Colombo Port City would provide a better assessment of the damage potential under various earthquake scenarios.

Acknowledgements

The authors extend gratitude to the University of Peradeniya and the Faculty of Engineering, Peradeniya, for their assistance and support. Appreciation goes to the Port Authority and management staff of the project for providing necessary data and access to Colombo Port City premises. Finally, the contributions of all academic staff of the Faculty of Engineering, Peradeniya, are gratefully acknowledged.

References

1. Chen, C. J. & Juang, C. H. (2000). Calibration of SPT- and CPT Based Liquefaction Evaluation Methods. *Geotechnical Special Publication* 97: 49–64.

2. Cubrinovski, M., Green, R. A., Allen, J., Ashford, S. A., Bowman, E., Bradley, B. A., Cox, B., Hutchinson, T. C., Kavazanjian, E., Orense, R. P., Pender, M., Quigley M. & Wotherspoon, L., (2010). Geotechnical Reconnaissance of the 2010 Darfield (Canterbury) Earthquake. *Journal of Bulletin of the New Zealand Society for Earthquake Engineering*. 43(4): 243-320.

3. Fukutake, K., & Yamamoto, Y. (1996). "Prediction of Liquefaction-Induced Ground Failures and Its Application." *Soils and Foundations*, 36(4), 51-64.

4. Kayen, R. E., Mitchell, J. K., Seed, R. B., Lodge, A., Nishio, S. & Coutinho, R. (1992). Evaluation of SPT-, CPT-, and Shear Wave-Based Methods for Liquefaction Potential Assessment using Loma Prieta Data. *Proceeding of the 4th Japan-U.S. Workshop on Earthquake-Resistant Des. Of Lifeline Fac. and Countermeasures for Soil Liquefaction* 1: 177–204.

5. Hazen, A. (1918). A Study of the Slip in the Calaveras Dam. *Journal of the Engineering News Record* 81(26): 1158-1164.

6. Ilangakoon, I. A. C. C. & Athapaththu, A. M. R. G., (2023). Estimation of Soil Liquefaction Potential in Colombo Port City (Sri Lanka) using Several Design Earthquakes. *Journal of the National Science Foundation of Sri Lanka* 51(1): 129-148.

7. Ishihara, K. (1993). "Liquefaction and Flow Failure During Earthquakes." *Geotechnique*, 43(3), 351-415.

8. Iwasaki, T., Tokida, K., Tatsuko, F., and Yasuda, S., (1978). A Practical Method for Assessing Soil Liquefaction Potential Based on Case Studies at Various Sites in Japan. *Proceedings of 2nd International Conference on Microzonation, San Francisco.* 885–896.

9. Juang, C. H. & Jiang, T., (2000). Assessing Probabilistic Methods for Liquefaction Potential Evaluation. *Journal of the Geotechnical Special Publication* 107:148–162.

10. Juang, C. H., Yuan, H., Le, D. H. & Ku, C. S. (2002). Assessing CPT-Based Methods for Liquefaction Evaluation with Emphasis on the Cases from the Chi-Chi, Taiwan, Earthquake. *Journal of the Soil Dynamic Earthquake Engineering* 22(3): 241–258.

11. Kumarasiri, H. C. & Abayakoon, S. B. S., (2008). Potential of Soil Liquefaction in Sri Lanka - A Dynamic Approach to the Mitigation of Natural Disasters. *Symposium – International Institute for Infrastructure Renewal and Reconstruction (IIIRR),* April 2008, Calgary, Canada. 10-12.

12. Robertson, P. K. & Wride, C. E. (1998). Evaluating Cyclic Liquefaction Potential using the Cone Penetration Test. *Journal of the Geotechnical Canada, Ottawa* 35(3)1; 442–459.

13. Seed, H. B. & Idriss, I. M. (1967). Analysis of Soil Liquefaction: Niigata Earthquake. *Journal of the Soil Mechanics and Foundation Division*, ASCE 93(3): 83-108.

14. Seed, H. B. and Idriss, I. M., (1971). Simplified Procedure for Evaluating Soil Liquefaction Potential. *Journal of the Soil Mechanics and Foundation Division*. 97(9):1249–1273.

15. Seed, H. B. & Idriss, I. M. (1982). Ground Motions and Soil Liquefaction During Earthquakes. *Earthquake Engineering Research Institute Monograph, Oakland, Calif.*

16. Seneviratne, H. N., Perera, L. R. K., Wijesundara, K. K., Dananjaya, R. M. S., & de S. Jayawardena U., (2020). Seismicity Around Sri Lanka from Historical Records and Its Engineering Implications. *Engineer: Journal of the Institution of Engineers, Sri Lanka* 53(2): 47–52.

17. Seneviatne, H. N., Wijesundara, K. K., Perera, L. R. K., & Dissanayake, P. B. R., (2016). A Macro Seismic Hazard Zonation for Sri Lanka. *Engineer: Journal of the Institution of Engineers, Sri Lanka* 53(3): 37–44.

18. Sonmez, H., (2003). Modification of the Liquefaction Potential Index and Liquefaction Susceptibility Mapping for a Liquefaction-Prone Area (Inegol, Turkey). *Journal of the Environ. Geo* 44: 862–871.

19. Yasuda, S., Harada, K., Ishikawa, K. & Kanemaru, Y. (2012). Characteristics of Liquefaction in Tokyo Bay Area by the 2011 Great East Japan Earthquake. *Journal of the Soils Foundation* 52(5): 793–810.

20. Youd, T. L. & Perkins, D. M. (1978). Mapping Liquefaction-Induced Ground Failure Potential, *Journal of the Geotechnical Engineering Division* 104: 443– 446.